



Cite this: *New J. Chem.*, 2021, 45, 8149

Insights into the existing form of glycolaldehyde in methanol solution: an experimental and theoretical investigation†

Yuehui Li, Yantao Shi,  Xuedan Song,  Zhengyan Zhao,  Naitian Zhang and Ce Hao *

Glycolaldehyde (HOCH₂CHO, GA), the simplest molecule containing both hydroxyl and aldehyde groups, is structurally the most elementary member of monosaccharide sugars, which may provide new clues for probing the origin of life on planets like the Earth. Uncovering the existing state of GA in solution systems is an important scientific issue. Generally, methanol is used as the main mobile phase in the liquid chromatography analysis of GA, but the state of GA existing in methanol solution remains unknown, thus making it difficult to analyse GA accurately. Herein, the state and dynamic equilibrium of GA in methanol solution were systematically studied by UV-visible spectroscopy, nuclear magnetic resonance (¹H-NMR) spectroscopy, liquid chromatography mass spectrometry (LC-MS) and density functional theory (DFT) calculations. The results demonstrated that the equilibrium component of GA in methanol solution is different from that in aqueous solution and that glycolaldehyde hemiacetal (GAHA) is a dominant component (>90%). Laying the foundation for experimental analysis, the transformation of different components at equilibrium was studied using DFT. The results confirm that hydrogen bonding-induced proton transfer occurs between the components at equilibrium. This work provides an important reference for the analysis of sugars and related compounds in various biochemical reactions.

Received 15th January 2021,
Accepted 6th April 2021

DOI: 10.1039/d1nj00252j

rsc.li/njc

Introduction

Glycolaldehyde (HOCH₂CHO, GA), also known as hydroxyacetaldehyde, is regarded as the smallest sugar molecule and the first monosaccharide molecule found in interstellar space.^{1–4} It may be closely related to the origin of life, making it an important research topic in biochemistry and geochemistry.^{5,6} In particular, GA and HCHO, small carbohydrate molecules, play an important role in the formation of complex biomolecules. For example, HCHO and GA are important building blocks in the construction of DNA nucleosides and DNA precursors.^{7–11} In terms of atmospheric chemistry, GA is a volatile oxygen-containing organic compound and is considered to be involved in the formation of secondary aerosols.¹² In addition, GA is a direct product of biomass combustion (or an intermediate product in the oxidation process of organic compounds)¹³ and regarded as a precursor of photochemical smog, which in turn affects climate change and human health.^{14–17} Thus, revealing the state of GA existing in different environments (gaseous, solid, and solution) is an important scientific issue.

The GA molecule contains two functional groups, a hydroxyl group and an aldehyde group. It has the dual properties of alcohol and aldehyde. Therefore, GA is chemically active and exhibits different forms in gas, solid and solution states. Particularly in solution, there is a complex dynamic equilibrium between different forms of GA.¹⁸ In recent years, the forms of GA in different states have been extensively investigated, as demonstrated in previous studies, by using a large number of experiments and theories.^{19–23} For example, it has been reported that gaseous GA exists in the form of monomer, connected by intermolecular hydrogen bonds, a stable configuration in the gaseous state. In the solid state, GA exists in the form of a dimer, and the most stable configuration of the dimer has been revealed to have a *P2₁/C* crystal structure.²⁴ Nevertheless, due to the strong solvation effect, GA in solution exists in more complex forms in dynamic equilibrium (usually in the form of isomeric monomers and dimers) when compared to gaseous or solid state.^{25–29} The form of GA that exists in aqueous solution has been extensively studied. Schnell *et al.* revealed a stable network structure composed of GA and water molecules by rotational spectroscopy and hydrogen bonding analysis.³⁰ Using experimental and theoretical methods, Kua *et al.* studied the equilibrium composition and corresponding mechanism of GA in aqueous solution, indicating that there are seven dimers and

State Key Laboratory of Fine Chemicals, School of Chemistry, Dalian University of Technology, Dalian 116024, People's Republic of China. E-mail: haoce@dlut.edu.cn

† Electronic supplementary information (ESI) available. See DOI: 10.1039/d1nj00252j

two monomers at the equilibrium state of GA in aqueous solution.²⁷ It is well known that methanol is usually used as the mobile phase in the liquid chromatography analysis of GA. However, up to now, the existing form and equilibrium state of GA in methanol solution still remain unknown, which makes the accurate analysis of GA difficult. Therefore, it is of great significance to study the form and dynamic equilibrium of GA in methanol solution.

Herein, the state and dynamic equilibrium of GA existing in methanol solution were studied by UV-visible spectroscopy, nuclear magnetic resonance (¹H-NMR) spectroscopy, liquid chromatography mass spectrometry (LC-MS) and density functional theory (DFT) calculation. The results suggest that the existing form of GA in methanol solution is obviously different from that in aqueous solution. In methanol solution, the main existing form is glycolaldehyde hemiacetal (GAHA), accounting for more than 90%. DFT studies reveal that hydrogen bond-induced proton transfer plays an important role in the transformation of different equilibrium components. This study provides an important basis for the analysis of sugars and related compounds in complex biochemical reactions.

Experimental

Materials and methods

Glycolaldehyde was purchased from Canada Toronto Research Chemicals (TRC). Deuterium methanol (CD₃OD) was purchased from Ningbo Rotation Meditech Co., Ltd. Chromatographic methanol was purchased from Tianjin Komeo Chemical Reagent Co., Ltd and used without further purification. All laboratory water was deionized water with a resistivity of 18 MΩ cm⁻¹.

Preparation of the standard solution of GA: A 0.5 M methanol solution and an aqueous solution of the GA dimer were prepared, kept stationary for 60 h, sealed and stored in a refrigerator (4 °C) to avoid light.

Characterization studies

UV-visible spectral absorption data were measured using a Cary-300 ultraviolet/visible spectrometer. The test range was 800–200 nm. The NMR spectral data were measured using an Avance II 500 M NMR instrument, and the peak areas were integrated using the MestreNova fitting software. ESI-MS experiments and high-resolution mass spectrometry were carried out using a LTQ linear ion trap mass spectrometer (Thermo, San Jose, CA, USA). An electrospray ion source (ESI⁺) was used to selectively monitor the molecular ion peaks of different substances. High performance liquid chromatographic (HPLC) separation was performed using a stainless steel column (C18, 150 mm×4.6 mm, 5 μm); the mobile phase was pure methanol, and the detector was an ultraviolet detector. The flow rate was 0.6 mL min⁻¹. The sample injection volume was 20 μL, and the column temperature was 35 °C.

Computational details

All calculations in this paper were carried out using the Gaussian 16 program package.³¹ All calculations are based on the density functional theory (DFT) method.³² Geometric optimization

of reactants, transition states and products is calculated at the level of the B3LYP-D3 (Grimme DFT-D3 corrected B3LYP) functional^{33,34} and 6-311G(d,p) basis sets.^{35,36} NMR calculations were performed using the gauge invariant atomic orbital (GIAO) approach. We also calculated the intrinsic reaction coordinates (IRCs) at the B3LYP/6-311G(d,p) level, from which we obtained the intermediates and products.³⁷ Moreover, considering the reaction of GA with methanol solution, all calculation processes are carried out in CH₃OH solvent, and the solvent model is SMD model; the calculated temperature is 298 K.³⁰ Furthermore, noncovalent interactions (NCIs) were analysed using the Multiwfn software package.³⁸

Results and discussion

According to previously reported literature, the form of GA existing in aqueous solution is complex; there are seven dimers and two monomers at the equilibrium state of GA in aqueous solution, and the main component is GA hydrate.²⁷ Moreover, dynamic equilibrium was also verified by the nuclear magnetic resonance (NMR) spectra (Fig. S1, ESI[†]). We firstly put forward some possible components of GA in methanol solution, as shown in Fig. 1. Notably, a hemiacetal reaction can take place between glycolaldehyde and methanol molecules at room temperature in methanol solution, and the main component is conjectured to be glycolaldehyde hemiacetal (GAHA).³⁹ Based on the above analysis, we could suppose that component 2 and monomer 5 react with methanol molecules to form new components 7 and 6 in methanol solution at room temperature (Fig. 1), which can be attributed to the hemiacetal reaction between the aldehyde group and hydroxyl group.

For better comparisons, experimental and theoretical NMR spectroscopy measurements were conducted to determine the different components derived from GA in methanol solution. The experimental NMR results shown in Fig. 2 demonstrate

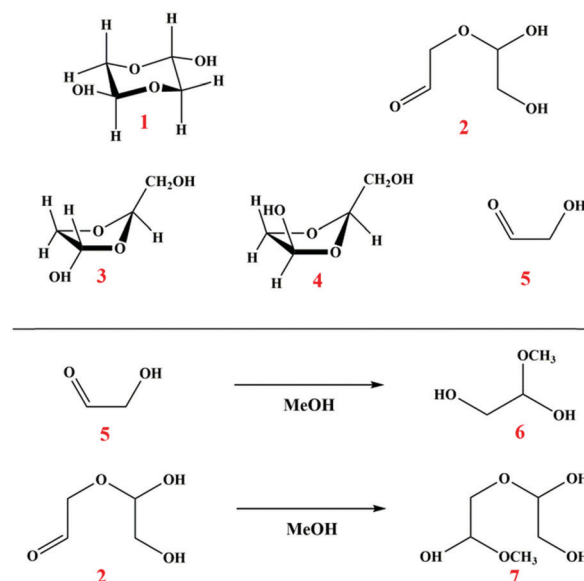


Fig. 1 Some possible components of GA in methanol solution.

that many peaks have been well assigned by combination with the compounds shown in Fig. 1, among which those with low contents and close chemical shifts are hardly determined to originate from monomers or dimers. To analyse the contents of different components, the chemical shifts of the characteristic functional groups can be used to identify specific components, and the peak area has been integrated using the Mestrenova fitting software. The peak corresponding to the chemical shift of 4.79 is due to the small amount of water in deuterated methanol. Obviously, it can be concluded that the content of GA monomer in methanol solution is lower than that in aqueous solution (Fig. S1, ESI[†]), which is attributed to the stronger affinity of the methoxy groups and higher content of GAHA formed in the reaction with the aldehyde groups. Moreover, the content of main component 6 was ~90%, which is consistent with that reported in previous literature.³⁹

To further study the equilibrium of GA in methanol solution, time-resolved ¹H-NMR was employed to analyze the content of different components in Fig. S3 (ESI[†]). The first data were recorded within 5 min of mixing, and they were recorded once in 2 h, as the reaction proceeded. After 60 h, samples were near equilibrium, and the final measurement was taken 65 h after mixing. The results revealed that the equilibrium contents of component 6 gradually increased and the concentration of GA dimer 1 gradually decreased as the reaction proceeded. After 60 h, the contents of components 1 and 6 changed slightly, suggesting the system achieved a dynamic equilibrium. Moreover, several concentrations of GA dimer (0.05 M, 0.1 M, 0.25 M, and 0.5 M) in methanol solution were measured by ¹H-NMR spectra as shown Fig. S4 and Table S1 (ESI[†]). The NMR data revealed that, with the increase in the concentration of the GA dimer, the equilibrium concentration of component 6 increased after reaching the dynamic equilibrium at about 60 h, while the concentration of GA dimer 1 decreased significantly. The results implied that the reactions proceed in the direction of GA hemiacetal 6, when the concentration of reactant GA dimer increases. Combined with the experimental results, we also theoretically predicted ¹H NMR spectrum through calculation based on the DFT study, as shown in Table 1, using which we

Table 1 ¹H NMR data of the different components of GA in methanol solution (experimental and calculated values), and the content of different components

Components NO.	Experimental value (ppm)	Computed value (ppm)	Components (%)
1	4.0, 4.7	3.5, 4.9	~1.23
2	4.1, 9.6	4.0, 9.9	~0.07
3	3.9, 5.1, 5.5	3.6, 5.4, 5.6	~2.31
4	4.1, 5.2, 5.5	3.9, 4.2, 5.6	~4.95
5	4.2, 9.6	4.4, 9.9	~0.54
6	3.4, 4.5	3.8, 4.7	~90.87
7	5.1	5.6	~0.03

can further confirm the various components of GA in methanol solution. As displayed in Table 1, the calculated chemical shifts are relatively consistent with the experimental observations, suggesting the rationality of our model for calculation (Fig. 3).

Liquid chromatography–mass spectrometry (LC–MS) was used to further determine the different components of GA in methanol solution. During the separation process, methanol was used as the mobile phase, but the components could not be well separated. The retention time of different components was kept at approximately 2.3 min, as displayed in Fig. S5 (ESI[†]). The molecular ion peaks of different components were recorded by mass spectra as shown in Table S2 (ESI[†]).

The components of 1, 2, 3, and 4 are isomers that cannot be distinguished by mass spectra owing to their same molecular weight (143.0135). The *m/z* values for [5 + Na]⁺, [6 + Na]⁺ and [7 + Na]⁺ are 83.0102, 115.0365 and 175.0578, respectively. Here, the difference in molecular weight between components 5 and 6 or the difference in the molecular weight of components 2 and 7 is precisely the molecular weight of methanol (*M* = 32), indicating that monomer 5 and dimer 2 contain aldehyde functional groups and react with methanol to form components 6 and 7.

From the above data, the composition and proportion of GA in methanol solution were obtained. We could conclude that the ring opening reaction of the GA dimer took place under the solvent effect; components 1, 2, 3, 4, and 5 are the same as the components in aqueous solution. However, components 6 and 7 are different. The main reason for this is that monomer 5 and

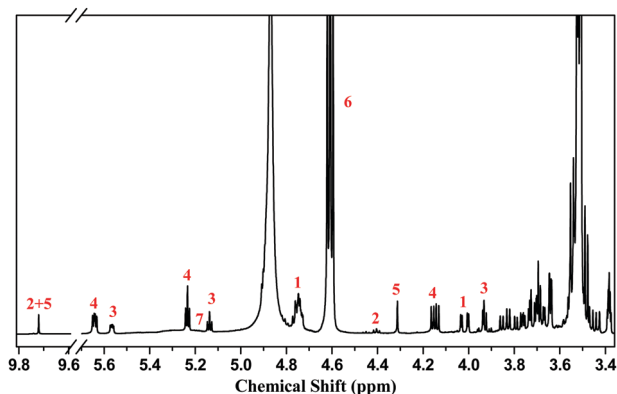


Fig. 2 ¹H-NMR spectra of GA in CD₃OD solution. Monomer peaks (5, 6), acyclic dimers and cyclic dimers (1, 2, 3, 4 and 7). The complete ¹H-NMR spectra are also provided in Fig. S2, ESI[†].

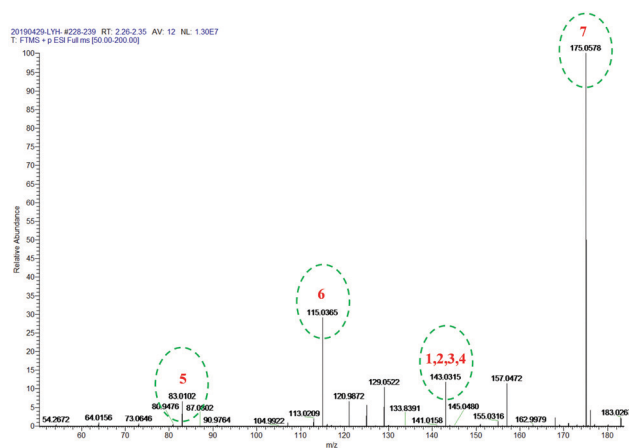


Fig. 3 Mass spectra of different components of GA in methanol solution.

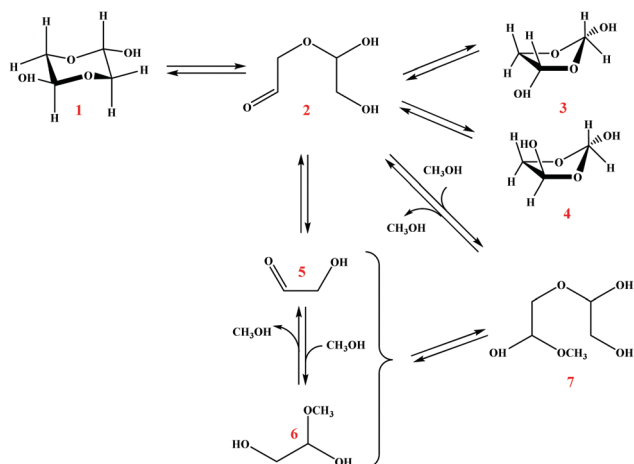


Fig. 4 The existence state and dynamic equilibrium diagram of GA in methanol solution at room temperature (298 K).

acyclic dimer 2 contain aldehyde functional groups and react with methanol molecules to form GAHA 6 and acyclic dimer 7, which is related to the hemiacetal reaction of methanol molecules.

To better comprehend the reaction process of the different components in methanol solution, the reaction paths were obtained, as shown in Fig. 4. At room temperature, the GA dimer is dissolved in aqueous solution or methanol solution, and the reaction is carried out in three steps, as discussed above. (1) Due to the hydrogen bond effect of the methanol solvent, the six-membered ring of the GA dimer first forms an open ring structure, and the C–O single bond is broken to form acyclic dimer 2, namely, the C4 compound containing a CHO group. (2) After ring opening, component 2 continues to form GA monomer 5 or cyclic dimers 3 and 4. (3) The GA monomer reacts with methanol molecules to form GAHA in methanol solution.

To better explore the possibility of the conversion between different components at room temperature, DFT calculation was used to explain the reaction mechanism from the kinetic point of view. Considering the effect of methanol solvation, we considered two molecules,⁴⁰ and the activation energy barriers of different reactions were obtained. As shown in Fig. 5, initial ring dimer 1 undergoes transformation to acyclic dimer 2, with a barrier of 16.5 kcal mol⁻¹. Acyclic dimer 2 can undergo ring closure to form cyclic dimers 3 and 4, and the barriers are 14.3 kcal mol⁻¹ and 12.5 kcal mol⁻¹, respectively. Acyclic dimer 2 can also be converted into monomer 5 with methanol solvent, and the barrier is 15.5 kcal mol⁻¹. The hemiacetal reaction of acyclic dimer 2 with methanol molecules leads to dimer 7, with a relatively low barrier of 6.1 kcal mol⁻¹. C–O fracture occurred in the conversion of the acyclic dimer 7 to monomers 5 and 6 due to the effect of the methanol solvent, and the barrier was 15.5 kcal mol⁻¹. Moreover, in the reaction of monomer GA with methanol, the barrier of the transformation of 5 to 6 is 17.2 kcal mol⁻¹. The results confirmed that the activation energy of the conversion between different components is low (<20 kcal mol⁻¹), indicating the conversion could occur between different components at room temperature. The calculation

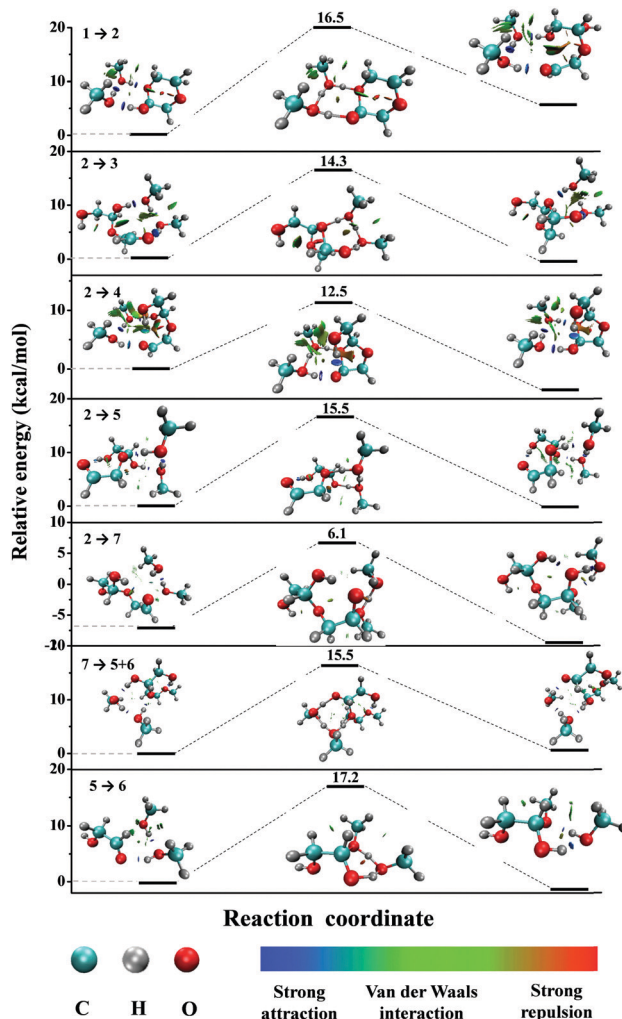


Fig. 5 Intrinsic reaction coordinate (IRC) path map of the reaction of GA in methanol solution from 1 to 2, 2 to 3, 2 to 4, 2 to 5, 2 to 7, 7 to 5, and 5 to 6. The reaction was analysed using the weak interaction NCI of Multiwfn software. Blue represents strong interactions, such as hydrogen bonds and halogen bond, green represents van der Waals forces, and red represents space resistance.

results suggest that dimer 1 converts to 2 due to the ring opening reaction of the hydrogen bond of solvent, component 2 transforms into 3, 4, 5, and 7 due to the solvent effect. It is obvious that the reaction between components 2 and 7 has a relatively low barrier of 6.1 kcal mol⁻¹, mainly from the reaction path of components 2 to 7. Finally, acyclic dimer 7 converts to components 5 and 6, and GA monomer 5 transforms into 6 through the solvent effect. This is consistent with the above mentioned suggesting that component 6 is the main equilibrium component in methanol solution.

To elucidate the cause for difference in reactions, noncovalent weak interaction hydrogen bonds were considered. Hydrogen bonds are special intramolecular or intermolecular interactions that are the most common, basic, important and weak.^{41,42} For example, they are an important part of carbohydrates, which maintain their conformation through intramolecular or intermolecular hydrogen bond competition.³⁹ Considering the effect

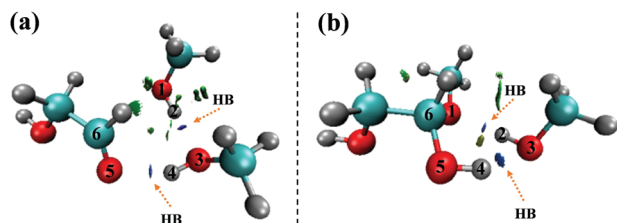


Fig. 6 The reaction path for 5 \rightarrow 6 of GA in methanol solution, (a) reactant and (b) product. The reaction was analysed by using the weak interaction NCI of Multiwfn software. Blue represents strong interactions, that is, hydrogen bonds, green represents van der Waals forces, and red represents space resistance.

of the hydrogen bonds (H \cdots O–H) on different components, the mechanism of hydrogen bond induced proton transfer was studied, as shown in the ESI† Fig. S6–S11. Additionally, we used Multiwfn software to analyse the noncovalent weak interaction (NCI) of the different reactions, as illustrated in Fig. 5. Blue represents strong interactions (hydrogen bonds and halogen bonds), green represents weak interactions (van der Waals forces), and red represents space resistance.^{43–46} At the same time, the bond length and bond angle of reactants and products have changed and are shown in the ESI† Tables S3–S8.

Considering the difference between the components of GA in methanol and aqueous solutions, component 6 is the main component in methanol solution. We focus on the chemical reaction energy barriers of monomer 5 transforming into component 6. As discussed above, the activation energy barrier is 17.2 kcal mol^{−1}. As displayed in Fig. 6 and Table 2, the bond length of H2–O3 changed from 1.82 Å to 0.97 Å, and the acting force changed from blue to green, indicating that the acting force changed from hydrogen bonds to covalent bonds. The bond length of H4–O5 changed from 1.92 Å to 0.98 Å, and the acting force changed from blue to green, indicating that the acting force changed from hydrogen bonds to covalent bonds. However, after the reaction occurred for 52 h, the bond length of O1–H2 changed from 0.98 Å to 1.89 Å, and the colour of the bond changed to blue, suggesting that the covalent bond changed to a hydrogen bond. The bond length of O3–H4 changed from 0.97 Å to 1.93 Å, and the colour of the bond changed to blue, indicating that the chemical bond broke and formed a hydrogen bond. Before the reaction, O5–C6 existed in

the form of a C=O double bond, and the bond length was 1.22 Å. After the reaction, the double bond of O5–C6 was saturated, and the bond length became 1.40 Å. The bond length of C6–O1 changed from 2.98 Å to 1.44 Å, and the colour between C6 and O1 changed from green to the colour of a covalent bond. At the same time, the bond angle of H2–O3–H4 changed from 93.4° to 75.8°, that of H4–O5–C6 changed from 118.8° to 107.5°, that of O5–C6–O1 changed from 94.4° to 107.5°, and that of C6–O1–H2 changed from 76.5° to 103.9°. Because of the hydrogen bond effect between the methanol molecule and GA monomer, the bond length and the bond angle changed obviously, and a new substance (GAHA) was formed. Overall, glycolaldehyde hemiacetal is the main component of GA in methanol solution at room temperature (298 K), while in aqueous solution it is mainly glycolaldehyde hydrate. Hydrogen bond induced proton transfer occurs between different equilibrium components.

Conclusions

In this paper, the state and dynamic equilibrium of GA existing in methanol solution was studied by UV-visible spectroscopy, ¹H-NMR spectroscopy, LC-MS and DFT calculations. The results show that the equilibrium composition of GA in methanol solution is different from that in aqueous solution. GA exists in the form of five dimers and two monomers at equilibrium in methanol solution, while previous reports suggest that GA exists as seven dimers and two monomers in aqueous solution. The main difference is that GAHA is a dominant component in methanol solution (>90%); however, GA hydrate is the main component (>70%) in aqueous solution. At the same time, we used DFT calculations to study hydrogen bond-induced proton transfer between different equilibrium components. The combination of experiments and theory provides the basis for the analysis of sugars and related compounds in complex biochemical reactions.

Conflicts of interest

There are no conflicts to declare.

Acknowledgements

This work was financially supported by the National Natural Science Foundation of China (Grant No. 21677029 and 21606040).

Notes and references

- 1 M. T. Beltrán, C. Codella, S. Viti, R. Neri and R. Cesaroni, *Proc. Int. Astron. Union*, 2010, **5**, 701–702.
- 2 J. M. Hollis, F. J. Lovas and P. R. Jewell, *Astrophys. J.*, 2000, **540**, 107–110.
- 3 J. K. Jørgensen, C. Favre, S. E. Bisschop, T. L. Bourke, E. F. van Dishoeck and M. Schmalzl, *Astrophys. J.*, 2012, **757**, 1–5.
- 4 M. K. Sharma, A. K. Sharma, M. Sharma and S. Chandra, *New Astron.*, 2016, **45**, 45–47.

Table 2 The bond length and angle of the 5 \rightarrow 6 reactant and product of GA in methanol solution

Parameters		Reactant	Product
Bond length (Å)	H2–O3	1.82	0.97
	O3–H4	0.97	1.93
	H4–O5	1.92	0.98
	O5–C6	1.22	1.40
	C6–O1	2.98	1.44
	O1–H2	0.98	1.89
Bond angle (°)	H2–O3–H4	93.4	75.8
	H4–O5–C6	118.8	107.5
	O5–C6–O1	94.4	107.5
	C6–O1–H2	76.5	103.9

- 5 A. K. Eckhardt, M. M. Linden, R. C. Wende, B. Bernhardt and P. R. Schreiner, *Nat. Chem.*, 2018, **10**, 1141–1147.
- 6 M. Haas, S. Lamour, S. B. Christ and O. Trapp, *Commun. Chem.*, 2020, **3**, 140.
- 7 S. A. Benner, H. J. Kim, M. J. Kim and A. Ricardo, *Cold Spring Harbor Perspect. Biol.*, 2010, **2**, 1–22.
- 8 F. M. Kruse, J. S. Teichert and O. Trapp, *Chemistry*, 2020, **26**, 14776–14790.
- 9 J. S. Teichert, F. M. Kruse and O. Trapp, *Angew. Chem., Int. Ed.*, 2019, **58**, 9944–9947.
- 10 A. Ricardo, M. A. Carrigan, A. N. Olcott and S. A. Benner, *Science*, 2004, **303**, 196.
- 11 R. Larralde, M. P. Robertson and S. L. Miller, *Proc. Natl. Acad. Sci. U. S. A.*, 1995, **92**, 8158–8160.
- 12 T. J. Johnson, R. L. Sams, L. T. Profeta, S. K. Akagi, I. R. Burling, R. J. Yokelson and S. D. Williams, *J. Phys. Chem. A*, 2013, **117**, 4096–4107.
- 13 R. J. Yokelson, R. Susott, D. E. Ward, J. Reardon and D. W. T. Griffith, *J. Geophys. Res.: Atmos.*, 1997, **102**, 18865–18877.
- 14 B. Camilla, S. T. Geoffrey and O. J. John, *J. Atmos. Chem.*, 2001, **39**, 171–189.
- 15 M. M. Galloway, A. J. Huisman, L. D. Yee, A. W. H. Chan, C. L. Loza, J. H. Seinfeld and F. N. Keutsch, *Atmos. Chem. Phys.*, 2011, **11**, 10779–10790.
- 16 Y. B. Lim, Y. Tan, M. J. Perri, S. P. Seitzinger and B. J. Turpin, *Atmos. Chem. Phys.*, 2010, **10**, 10521–10539.
- 17 M. J. Perri, S. Seitzinger and B. J. Turpin, *Atmos. Environ.*, 2009, **43**, 1487–1497.
- 18 H. Michelsen and P. Klaboe, *J. Mol. Struct.*, 1969, **4**, 293–302.
- 19 J. Altnoder, J. J. Lee, K. E. Otto and M. A. Suhm, *ChemistryOpen*, 2012, **1**, 269–275.
- 20 G. C. S. Collins and W. George, *J. Chem. Soc. B*, 1971, 1352–1355.
- 21 M. L. Senent, *J. Phys. Chem. A*, 2004, **108**, 6286–6293.
- 22 V. A. Yaylayan, S. Harty-Majors and A. A. Ismail, *Carbohydr. Res.*, 1998, **309**, 31–38.
- 23 S. Zinn, C. Medcraft, T. Betz and M. Schnell, *Angew. Chem., Int. Ed.*, 2016, **55**, 5975–5980.
- 24 V. Mohaček-Grošev, B. Prugovečki, S. Prugovečki and N. Strukan, *J. Mol. Struct.*, 2013, **1047**, 209–215.
- 25 G. K. Glushonok, T. G. Glushonok and O. I. Shadyro, *Kinet. Catal.*, 1998, **41**, 682–686.
- 26 J. Kua, M. M. Galloway, K. D. Millage, J. E. Avila and D. O. De Haan, *J. Phys. Chem. A*, 2013, **117**, 2997–3008.
- 27 C. I. Stassinopoulou and C. Zioudrou, *Tetrahedron*, 1972, **28**, 1257–1263.
- 28 J.-R. Aviles-Moreno, J. Demaison and T. R. Huet, *J. Am. Chem. Soc.*, 2006, **128**, 10467–10473.
- 29 P. Wang, Y. Hu, H. Zhan and J. Chen, *RSC Adv.*, 2017, **7**, 6242–6250.
- 30 C. Perez, A. L. Steber, B. Temelso, Z. Kisiel and M. Schnell, *Angew. Chem., Int. Ed.*, 2020, **59**, 8401–8405.
- 31 M. J. Frisch; G. W. Trucks; H. B. Schlegel; G. E. Scuseria; M. A. Robb; J. R. Cheeseman; G. Scalmani; V. Barone; G. A. Petersson; H. Nakatsuji; X. Li; M. Caricato; A. V. Marenich; J. Bloino; B. G. Janesko; R. Gomperts; B. Mennucci; H. P. Hratchian; J. V. Ortiz; A. F. Izmaylov; J. L. Sonnenberg; D. WilliamsYoung; F. Ding; F. Lipparini; F. Egidi; J. Goings; B. Peng; A. Petrone; T. Henderson; D. Ranasinghe; V. G. Zakrzewski; J. Gao; N. Rega; G. Zheng; W. Liang; M. Hada; M. Ehara; K. Toyota; R. Fukuda; J. Hasegawa; M. Ishida; T. Nakajima; Y. Honda; O. Kitao; H. Nakai; T. Vreven; K. Throssell; J. A. Montgomery Jr.; J. E. Peralta; F. Ogliaro; M. J. Bearpark; J. J. Heyd; E. N. Brothers; K. N. Kudin; V. N. Staroverov; T. A. Keith; R. Kobayashi; J. Normand; K. Raghavachari; A. P. Rendell; J. C. Burant; S. S. Iyengar; J. Tomasi; M. Cossi; J. M. Millam; M. Klene; C. Adamo; R. Cammi; J. W. Ochterski; R. L. Martin; K. Morokuma; O. Farkas; J. B. Foresman and D. J. Fox, *Gaussian16 Revision B.01*, Gaussian Inc., Wallingford CT, 2016.
- 32 A. D. Becke, *J. Chem. Phys.*, 1993, **98**, 5648–5652.
- 33 S. Grimme, *J. Comput. Chem.*, 2006, **27**, 1787–1799.
- 34 T. Schwabe and S. Grimme, *Phys. Chem. Chem. Phys.*, 2007, **9**, 3397–3406.
- 35 R. Krishnan, J. S. Binkley, R. Seeger and J. A. Pople, *J. Chem. Phys.*, 1980, **72**, 650–654.
- 36 A. D. McLean and G. S. Chandler, *J. Chem. Phys.*, 1980, **72**, 5639–5648.
- 37 A. V. Marenich, C. J. Cramer and D. G. Truhlar, *J. Phys. Chem. B*, 2009, **113**, 6378–6396.
- 38 T. Lu and F. Chen, *J. Comput. Chem.*, 2012, **33**, 580–592.
- 39 M. Dusselier, P. V. Wouwe, S. D. Smet, R. D. Clercq, L. Verbelen, P. V. Puyvelde, F. E. D. Prez and B. F. Sels, *ACS Catal.*, 2013, **3**, 1786–1800.
- 40 K. S. Thanthiriwatte, J. R. Duke, V. E. Jackson, A. R. Felmy and D. A. Dixon, *J. Phys. Chem. A*, 2012, **116**, 9718–9729.
- 41 N. V. Belkova, L. M. Epstein, O. A. Filippov and E. S. Shubina, *Chem. Rev.*, 2016, **116**, 8545–8587.
- 42 M. S. Taylor and E. N. Jacobsen, *Angew. Chem., Int. Ed.*, 2006, **45**, 1520–1543.
- 43 J. Contreras-Garcia, W. Yang and E. R. Johnson, *J. Phys. Chem. A*, 2011, **115**, 12983–12990.
- 44 E. R. Johnson, S. Keinan, P. Mori-Sánchez, J. Contreras-García, A. J. Cohen and W. Yang, *J. Am. Chem. Soc.*, 2010, **132**, 6498–6506.
- 45 A. S. Mahadevi and G. N. Sastry, *Chem. Rev.*, 2016, **116**, 2775–2825.
- 46 A. Otero-de-la-Roza, E. R. Johnson and J. Contreras-Garcia, *Phys. Chem. Chem. Phys.*, 2012, **14**, 12165–12172.